

Optical inhomogeneities of the cloud base

V.S. Shamanaev, I.E. Penner, and G.P. Kokhanenko

*Institute of Atmospheric Optics,
Siberian Branch of the Russian Academy of Sciences, Tomsk*

Received October 4, 2006

In the experiments on laser sounding of the cloud base (CB), CB height horizontal distributions, the gradient of the scattering coefficient in the cloud boundary, and the vertically averaged scattering coefficient have been measured. Further, the energy spectra of the parameters and their fluctuations were calculated. The shape of the spectra was shown to be qualitatively close to that measured using an airborne lidar at the cloud top. Even the presence of strongly inhomogeneous CB with the step-wise height variations and precipitations does not change the situation.

It is known that both the cloud top (CT) and cloud base (CB) have inhomogeneous structure. It is also related to both geometric inhomogeneities, i.e., fluctuations of CT and CB, and optical ones, for example, coefficient of light scattering. Although the geometric parameters are calculated from the optical measurements as well.

Cloud base was one of the first objects for laser sounding: it is easy to record lidar returns, and there are clouds on sky practically always. Moreover, quite wide international experiment ECLIPS (Experimental Cloud Lidar Pilot Study) was carried out.¹ About 15 lidar research groups from Australia to Canada, including Russia, sounded clouds at coordinated time. However, no unified system for data processing and representation was used. The lidar signals were processed by one or another algorithm were represented more often as histograms of probability of occurrence of different values of the parameters under study. It was quite difficult to compare the results of different groups, especially in the presence of broken sequences of lidar returns, as is often the case with field experiments.

So, in studying the cloud top, we have passed to the relative measured parameters, for example, the variations of the cloud height.^{2,3} Following this technique, the trend is removed from the measurement sample, then standard deviation is calculated, and the sample is normalized to it. Subsequent processing is applied to this transformed sample as to a stationary random process.

In the described experiment, at vertical upward sounding of the cloud base, we compared the simultaneous behavior of the CB height, scattering coefficient σ at CB, and the gradient of σ along the vertical direction. Let us remind that, according to the meteorological dictionary,⁴ clouds are “the systems of suspended products of condensation of water vapor – water droplets or ice crystals, or both of them, in the atmosphere (not just near the ground surface). As cloud elements grow and their falling velocity increases, they fall out from the cloud as precipitation. The droplet diameters in clouds are

from fractions of micrometer to 200 μm . The liquid water content in clouds is from some hundredth of a gram to several grams per 1 m^3 of the cloud air.”

The vertical distribution of σ has, in general, a predetermined shape, but under strong effect of random component. The horizontal distribution of σ at any fixed height is mainly random. The cloud base is considered as a several tens of meters thick layer starting from the height above the ground (or the distance from the lidar), at which water droplets (or crystals) occur in the atmosphere, and the scattering coefficient exceeds that of the free atmosphere under the cloud. Really, the thickness of this layer is set quite conventionally (as, for example, the thickness of the atmospheric boundary layer), but, as applied to laser sounding, it is logical to refer it to the depth of penetration of the sounding pulse into the cloud.

The scattering coefficient of the cloud was calculated using the Kovalev’s asymptotic algorithm⁵:

$$\sigma(r) = \frac{F(r)r^2}{2 \left[\int_{r_0}^{\infty} F(x)x^2 dx - \int_{r_0}^r F(x)x^2 dx \right]}, \quad (1)$$

where $F(r)$ is the power of the return signal corresponding to the distance r from the lidar, r_0 is the distance to the cloud base. The term “cloud base height” is ambiguous. Its numerical value varied in some limits even for the same return signal depending on the selected criterion. Earlier we have analyzed this fact.⁶ The “microphysical” boundary is accepted in Eq. (1) as the distance to the cloud base r_0 , when the cross section of backscattering of the cloud particles begins to exceed the cross section of backscattering of the atmosphere, and the derivative the return signal changes its sign for the first time. This enables one to slightly increase the optical thickness of the cloud sounded and thus to improve the accuracy of measurements of the scattering coefficient.

The infinity symbol “ ∞ ” means asymptotic regime, when the return signal drops down to zero in

the cloud depth. Experimental practice has shown that the “infinite” depth of sounding for a relatively dense lower layer clouds can be replaced with the maximum depth r_{\max} , at which the recording system still detects the signal.

It was shown in Ref. 6 that the values $\sigma(r)$ calculated from the lidar signals at the depth in the cloud equal to the half of the maximum depth of sounding, i.e., up to $0.5R_2 = 0.5(r_{\max} - r_0)$ are quite reliable. (The notations are used corresponding to that used in Ref. 6).

Therefore, the mean over depth scattering coefficient was proposed for describing the horizontal structure of the cloud base using just the scattering coefficient:

$$\hat{\sigma} = \frac{1}{0.5R_2} \int_{r_0}^{r_0+0.5R_2} \sigma(x) dx. \quad (2)$$

It is proposed to consider this value as the scattering coefficient at the given point of the cloud base. It seems sufficiently natural and self-organizing, because the denser is the cloud, the less is the depth of penetration of the beam and the less is the depth of $\hat{\sigma}$ averaging.

Another parameter suitable for the description of the cloud base is the gradient of the scattering coefficient. It is the measure of the CB fuzziness. Direct measurements of the vertical distribution of the optical density of clouds, see for example Ref. 7, revealed that the scattering coefficient first increases, and then, closer to the cloud top, begins to decrease. Of course, all this is modulated by the fluctuation processes. According to Ref. 6, in approximation of linear increase of the scattering coefficient we have that

$$\text{grad}\sigma(r) = \mu_\sigma = \frac{1}{2(r_m - r_0)^2} \frac{2r_0 - r_m}{r_m}. \quad (3)$$

Indeed, if $\sigma(r) = \mu_\sigma(r - r_0)$ for $r > r_0$, the power of the return signal from the cloud by canonic equation of laser sounding in the single scattering approximation is

$$F(r) = \frac{A}{r^2} \mu_\sigma (r - r_0) \exp[-\mu_\sigma (r - r_0)^2]; \quad (4)$$

$$\sigma(r) = \mu_\sigma (r - r_0), \quad r > r_0.$$

It is accepted here that scattering in the cloud depth is much stronger than that in the atmosphere under the cloud. The constant A includes all instrumentation and atmospheric constants, which are not essential at that moment for understanding the considered problems.

Let us remind that two competing processes form the return signal: its increase due to the growth of the scattering coefficient $\mu_\sigma(r - r_0)$ and the Bouguer attenuation due to the factor $\exp[-\mu_\sigma(r - r_0)^2]$. The result is the well-known maximum of the return signal at the depth in the cloud $r_m > r_0$. (One usually

uses it as a criterion in measuring the distance to the cloud boundary). Taking logarithm of Eq. (4) and its derivative with respect to r , we solve the problem on finding the extreme at the point r_m . Then we obtain Eq. (3). If one considers the S -function $S(r) = F(r)r^2$ instead of the signal power $F(r)$, Eq. (3) is simplified to $\mu_\sigma = 0.5(r_m - r_0)^{-2}$.

Let us consider the obtained experimental results. Sounding of stratus cloudiness was carried out by means of a “Makrel-2” lidar described many times, however, without using polarization. The specifications concerning the solved problem are the following: the standard wavelength of radiation was 532 nm, the laser pulse duration at the level of 0.35 was 15 ns, the step of 7-digit analog-to-digital converter in the considered experiment was 10 ns. Thus, the spatial resolution of the lidar was 1.5 m, the repetition rate of the laser pulses was 1 Hz.

In addition we have monitored the speed of cloud motion. For that we measured travel time of well pronounced inhomogeneities in the cloud field across a fixed field-of-view of a video camera. The cloud base height was measured with the lidar itself. Then a trivial trigonometric task was completed to calculate the speed of cloud motion. All this enabled us to estimate the horizontal sizes of the cloud inhomogeneities.

The computer algorithms we used in selecting the points r_0 and r_m have been described in Refs. 2 and 3. These are based on a successive looking through of the signal points, with the step of digitization by an ADC, taking into account monotonicity of the returns and their excess over some threshold.

Let us note that the functionals $\hat{\sigma}$ and μ_σ are obtained from the same lidar signal. But one can consider them as independent, because $\hat{\sigma}$ is the integral value, and μ_σ is the differential one. Therefore, one can compare them in the subsequent statistical analysis as two independent samples.

The results obtained by preprocessing the return signals from a 136-km long cloud field are shown in Fig. 1.

Preliminary analysis of this experiment makes it possible to divide the total time series of measurements into 3 parts with the local time of performing the sounding in the intervals 18:30–19:00, 19:00–19:50, and 19:50–20:30 for subsequent comparison of statistical estimates of the optical characteristics of cloudiness. The main criteria are the visually observed variance of the CB height (Fig. 1a) and the general two-dimensional pattern of the CB field in this experiment (it is not shown in Fig. 1a in order to not overload it). Rain with slant falling band, due to wind, was observed both by means of the lidar and visually before approximately 18:55.

Absolute change of the CB height reaches here 300 m. However, another situation is with the depth mean value $\hat{\sigma}$ in the cloud boundary. Its standard deviation essentially changes during the experiment.

For three parts selected according to the general physical features, $\delta\hat{\sigma} = \Delta\sigma/\bar{\sigma}$, i.e., variation is equal to 67, 29, and 47% (changes quite noticeable).

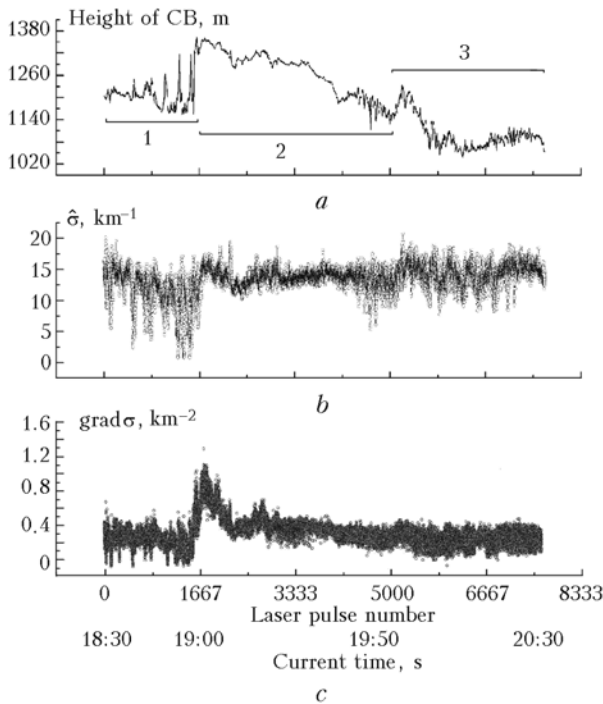


Fig. 1. Sounding of the 136-km long stratus cloud base: (a) horizontal profile of the CB height; (b) profile of the mean scattering index $\hat{\sigma}$; (c) profile of the gradient of the scattering angle μ_σ .

Mathematical expectation remains practically constant, that is seen even visually. The same is related to the gradient of the scattering coefficient μ_σ . It increases step-wise by 4 to 5 times in the region of a sharp change of the CB (it is approximately 1667-th laser shot), but on the other hand, its fluctuations decrease to 33%. In the parts before and after the jump, $\delta\mu_\sigma$ changes not very strongly (the variation is 70–80%).

Let us apply the fast Fourier transform, which showed its usefulness in observation of the cloud top,^{2,3} to the cloud base. Our purpose was to obtain the energy spectrum of fluctuations of one or another physical parameter as a function of spatial wavelength. Calculations were carried out by means of the Turbo Pascal Numerical Methods Toolbox software package. This is already a secondary processing of the lidar returns.

Figure 2 has been plotted using the total data set of more than two hour long sounding, i.e., about 8000 laser shots. Fluctuations of both $\hat{\sigma}$ and $\text{grad}\sigma$ in Fig. 2a, in general, fulfill the power law. But only $\text{grad}\sigma$ corresponds to the canonic power index of “–5/3”, and the functional $\hat{\sigma}$ changes the power of its fluctuation by the dependence “–6/3”, i.e., decreases noticeably faster. The confidence interval is shown on the curve of fluctuations of $\text{grad}\sigma$ at the place of break of the spectrum at the wavelengths of the processes inside the cloud with the scale of spatial wavelengths of 200–400 m (i.e., $f \sim 0.1$ Hz). It shows that this peak is quite significant and reflects the presence of the inner processes in the CB.

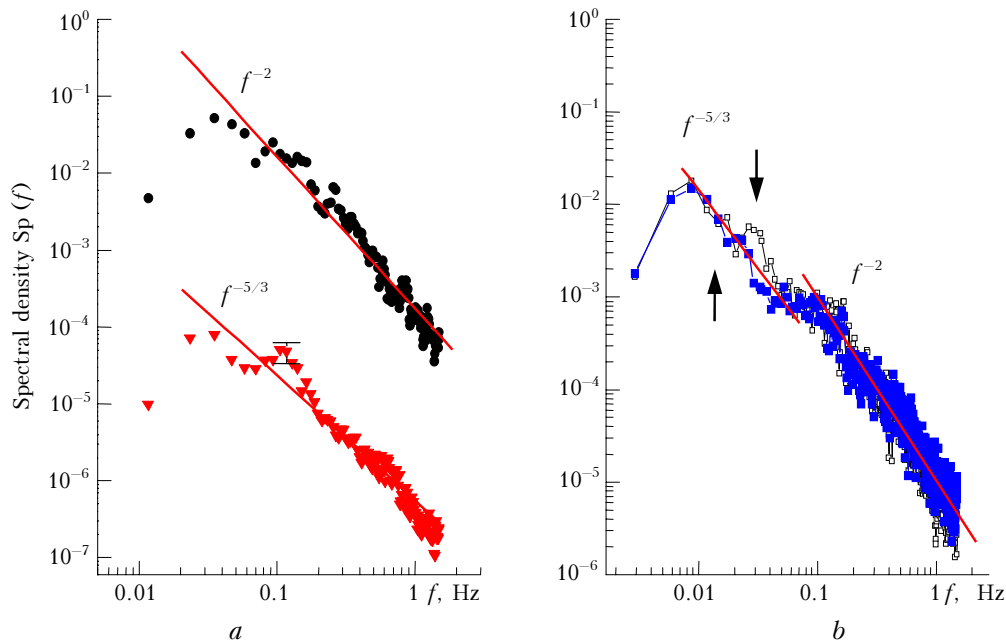


Fig. 2. Energy spectra of fluctuations of the parameters of cloudiness: (a) frequency spectrum of fluctuations of the values of the scattering coefficient $\hat{\sigma}$ (circles) and the gradient of the scattering coefficient (triangles); solid line is power law; (b) mutually normalized spectra of fluctuations of the scattering coefficient and the height of cloud base. Light squares correspond to scattering coefficient $\hat{\sigma}$; dark squares correspond to height of CB; solid line is approximations of the spectrum by power law. Arrows mark the spectrum break.

Let us remind that spatial wavelengths λ are related with the physical pulse repetition rate f by the measured cloud motion velocity v , and $\lambda = v/f$. The wind velocity at the cloud base was 20 m/s (one can consider them as a passive admixture), the laser operated with the frequency of 1 Hz.

The spectral densities of fluctuations of $\hat{\sigma}$ and H_{CB} are reduced to the general scale for qualitative comparison (Fig. 2*b*). It is seen that both spectra can be divided into two parts with different spatial scales, which have the exponents of the power dependence “ $-5/3$ ” and “ $-6/3$ ”.

This exponent in the region of higher frequencies (fractions of Hz, or the wavelengths of 250–20 m) is equal to “ -2 ”, that is more characteristic of turbulence developing inside the cloud layer.⁸ In the range of lower frequencies (0.05–0.008 Hz or the wavelengths 400–2500 m) this exponent is closer to the canonic value “ $-5/3$ ”, that is characteristic of single-dimensional fluctuations, which are in equilibrium state in the inertial interval of the spatial scales of turbulence. The range of frequency division lies in the range of spatial scales of the order of 200 to 400 m, that corresponds to the mean geometric thickness of the cloud layer⁴ (let us remind that there were strato-cumulus clouds). Let us also note the characteristic scale of the order ~ 600 m, well pronounced in the spectrum of fluctuations of the scattering coefficient $\hat{\sigma}$. It has the

shift to the higher frequency range in comparison with the same characteristic scale of fluctuations of H_{CB} , which is the external scale of turbulence relative to it.

Spectral densities of fluctuations of the considered geometrical and optical characteristics are shown in Fig. 3 separately for three parts (see Fig. 1*a*). Before 7 p.m., when the cloud base was very unstable, all the three parameters under study fluctuated approximately according to the same law, so that all spectra coincided. This law is quite far from the power law, because all curves are slightly convex in this double logarithmic scale. Then during the experiment, the CB height had the tendency to decrease, but its spontaneous break-like changes stopped and the fluctuation spectrum of the CB height became close to the “ $-5/3$ ” power law in the frequency range (i.e., also the spatial wavelengths of the size of inhomogeneities), which was determined by the length of even shortened samples, but not by the total data array as in Fig. 2. However fluctuations of the mean scattering coefficient and the gradient of the scattering coefficient kept their shapes different from the canonic power law. Nevertheless, fluctuations of the considered parameters of the cloud base for the total array of lidar signals (see Fig. 2) follow, in general, the power law that coincides with the data obtained for the cloud top.^{2,3}

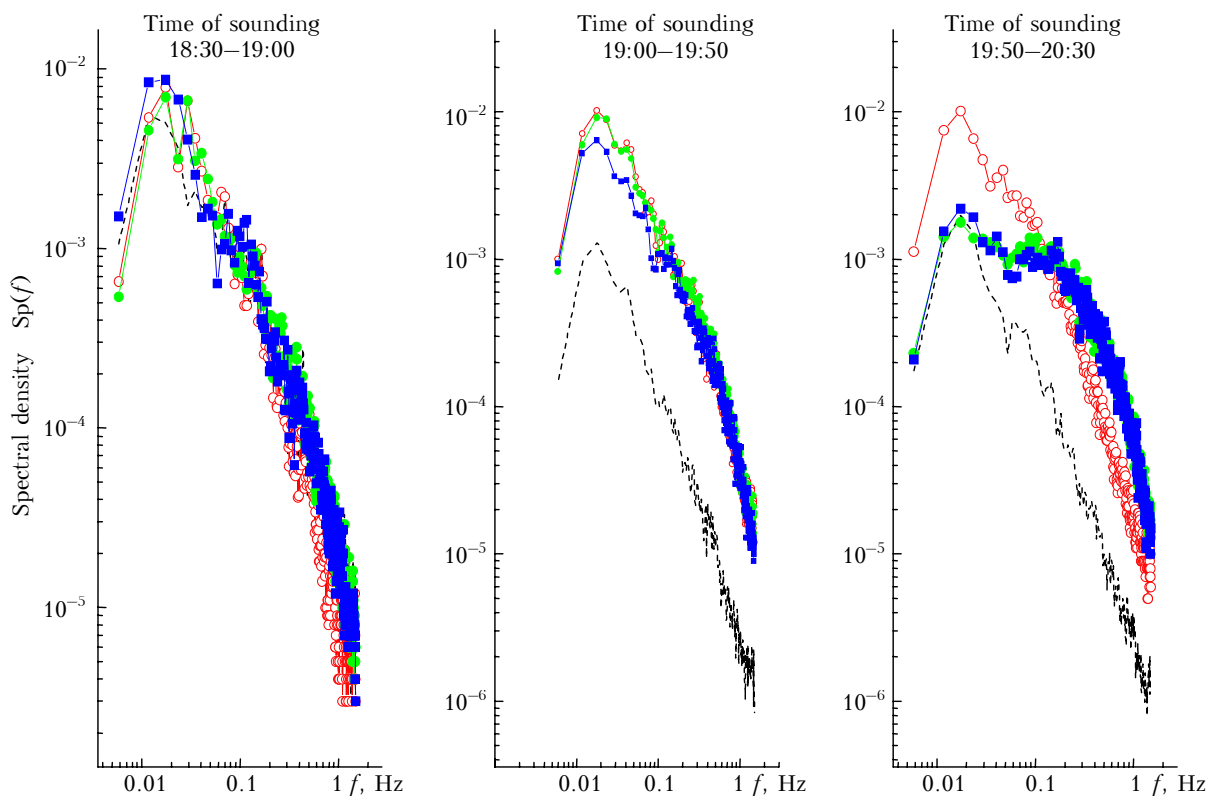


Fig. 3. Energy spectra of fluctuations of the parameters of cloudiness for three time intervals (see Fig. 1) of the experiment. Dotted line is height of CB, light circles are for scattering coefficient $\hat{\sigma}$; dark squares are for $\text{grad}\sigma(r)$.

Acknowledgement

The study was supported in part by the ISTC (grant No. B-1063).

References

1. C.M. Platt, S.A. Young, A.I. Carswell, S.R. Pal, M.P. McCormic, D.M. Winker, M. DelGuasta, L. Stefanutti, W.L. Eberhard, M. Hardesly, R.N. Flamant, R. Valentin, B. Forgan, G.G. Gimmetstad, H. Jager, S.S. Khmelevtsov, I. Kolev, B. Kaprielov, Lu Da-ren, K. Sassen, V.S. Shamanaev, O. Uchino, Y. Mizuno, U. Wandinger, C. Weitkamp, A. Ansmann, and C. Wooldridge, *Bull. Amer. Meteorol. Soc.* **75**, No. 9, 1635–1654 (1994).
2. I.E. Penner and V.S. Shamanaev, *Atmos. Oceanic Opt.* **12**, No. 12, 1095–1097 (1999).
3. I.E. Penner, G.P. Kokhanenko, and V.S. Shamanaev, *Atmos. Oceanic Opt.* **13**, No. 4, 348–354 (2000).
4. S.P. Khromov and L.I. Mamontova, *Meteorological Dictionary* (Gidrometeoizdat, Leningrad, 1963), 620 pp.
5. V.A. Kovalev, in: *Tr. Gl. Geofiz. Obs.*, Issue 321, 128–133 (1973).
6. V.S. Shamanaev, *Atmos. Oceanic Opt.* **5**, No. 7, 444–447 (1992).
7. A.L. Kosarev, I.P. Mazin, A.N. Nevzorov, and V.F. Shugaev, *Tr. Tsentr. Aerol. Obs.*, Issue 124 (1976), 167 pp.
8. N.K. Vinichenko, N.Z. Pinus, S.M. Shmeter, and G.N. Shur, *Turbulence in the Free Atmosphere* (Gidrometeoizdat, Leningrad, 1976), 288 pp.